

H-FedSN: Personalized Sparse Networks for Efficient and Accurate Hierarchical Federated Learning for IoT Applications

Jiechao Gao*

Department of Computer Science
University of Virginia
Charlottesville, VA, USA
jg5ycn@virginia.edu

Yuangang Li*

Thomas Lord Department of Computer Science
University of Southern California
Los Angeles, CA, USA
yuangang@usc.edu

Yue Zhao†

Thomas Lord Department of Computer Science
University of Southern California
Los Angeles, CA, USA
yzhao010@usc.edu

Brad Campbell†

Department of Computer Science
University of Virginia
Charlottesville, VA, USA
bradjc@virginia.edu

Abstract—The proliferation of Internet of Things (IoT) has increased interest in federated learning (FL) for privacy-preserving distributed data utilization. However, traditional two-tier FL architectures inadequately adapt to multi-tier IoT environments. While Hierarchical Federated Learning (HFL) improves practicality in multi-tier IoT environments by multi-layer aggregation, it still faces challenges in communication efficiency and accuracy due to high data transfer volumes, data heterogeneity, and imbalanced device distribution, struggling to meet the low-latency and high-accuracy model training requirements of practical IoT scenarios. To overcome these limitations, we propose H-FedSN, an innovative approach for practical IoT environments. H-FedSN introduces a binary mask mechanism with shared and personalized layers to reduce communication overhead by creating a sparse network while keeping original weights frozen. To address data heterogeneity and imbalanced device distribution, we integrate personalized layers for local data adaptation and apply Bayesian aggregation with cumulative Beta distribution updates at edge and cloud levels, effectively balancing contributions from diverse client groups. Evaluations on three real-world IoT datasets and MNIST under non-IID settings demonstrate that H-FedSN significantly reduces communication costs by 58 to 238 times compared to HierFAVG while achieving high accuracy, making it highly effective for practical IoT applications in hierarchical federated learning scenarios.

Index Terms—Hierarchical Federated Learning, Communication Efficiency, IoT, Bayesian Aggregation

I. INTRODUCTION

Incorporating advanced intelligence into ubiquitous Internet of Things (IoT) devices can enable applications such as personal healthcare [1] and smart cities [2]. Federated Learning (FL), known for its ability to manage distributed data sources while preserving data privacy [3], may be considered for use in IoT environments. However, conventional two-tier

FL algorithms [4], [5], [6] generally employ simplistic star network topologies, which are impractical for real-world IoT applications, as most IoT settings inherently operate within three-tier architecture. For example, in smart city surveillance scenarios [7], numerous IoT devices, such as surveillance cameras, are distributed across different buildings. The servers within each building normally first aggregate the data from the local sensors and then connect to the central cloud server for collaborative training. Similarly, in smart agriculture scenarios [8], numerous IoT devices, such as sensors and drones, are distributed across extensive farming areas. Each device locally processes data to analyze conditions such as soil moisture and crop health. The servers within each farm normally first aggregate the model parameters from these devices and then connect to the regional processing center’s cloud server for collaborative training. Therefore, traditional two-tier FL needs to be adapted to better fit the three-tier architecture in real-world IoT applications.

Compared to traditional two-tier FL, the Hierarchical Federated Learning (HFL) architecture is more practical and suitable for multi-tier environments typical of IoT settings due to its inherent multi-level structure, which aligns better with the layered processing needs of these systems. However, HFL must also overcome communication and model accuracy challenges to establish desirable IoT environments. Bandwidth and latency critically affect HFL’s performance, as the quality of communication at each tier directly influences the overall system’s efficiency. For instance, in the HierFAVG algorithm proposed by Liu et al., [9], which features an HFL architecture, the communication cost can be substantial due to the frequent and voluminous data exchanges required among devices (note that we treat one device as one client), edge servers, and the cloud. On the other hand, in realistic IoT environments,

*Equal contribution.

†Corresponding authors.

clients are normally under the condition of significantly non-IID conditions and also suffer from imbalanced device/data distribution, which causes substantial accuracy drops [10]. Therefore, it is crucial to develop effective communication strategies within HFL that not only reduce latency and bandwidth consumption but also maintain comparable model accuracy, ensuring high performance for IoT systems [11].

Although many methods [12], [13], [14] have been proposed to address communication and accuracy problems within conventional two-tier FL, directly applying these methods to a more realistic IoT setting (e.g., three-tier HFL) remains challenging and may result in performance degradation. For instance, traditional communication efficiency enhancement algorithms in two-tier FL [12], [13], [15] use block coordinate gradient descent, quantization, and asynchronous updates to reduce the amount of data transmitted during training. However, they still need clients to upload substantial model parameters, and the communication cost is not significantly reduced. Furthermore, there is a lack of research on how to apply FL communication algorithms to the HFL architecture. And also, methods that enhance communication efficiency may also compromise model accuracy [12], [16].

While many methods exist to improve model accuracy in two-tier FL, personalized federated learning algorithms are particularly suitable for IoT environments due to their ability to handle data heterogeneity, a prevalent challenge in IoT settings. Specifically, approaches such as those proposed in [17], [14], [18] improve accuracy by allowing local model adjustments based on client-specific data while leveraging shared knowledge, and these algorithms can be readily integrated into three-tier HFL architectures as they primarily involve client-side personalization adjustments. However, while these algorithms satisfy accuracy demands, they often do not optimize communication efficiency. Applying these techniques in a more realistic IoT setting (e.g., three-tier HFL) would still incur high communication costs, thereby affecting the overall IoT system performance. Thus, there is a pressing need to develop algorithms that can achieve high communication efficiency while maintaining model accuracy within the HFL.

In this paper, we propose H-FedSN, specifically designed for real-world IoT environments to achieve low communication costs and high accuracy in the HFL architecture. Our approach centers on a personalized, structured sparse model for each client, as shown in Fig. 1. Clients start with an identical neural network with frozen weights and train a corresponding binary (0,1) mask network. This binary mask network has the same structure as the original neural network. Applying this binary mask to the original network determines which connections to retain or prune, thereby creating a sparse network. The mask network consists of shared layers and personalized layers. Shared layers participate in global aggregation, becoming identical across all clients after training. Personalized layers are trained on client-specific data, remain local, and do not participate in global aggregation, resulting in unique layers for each client. H-FedSN significantly reduces communication costs by at least 58 times

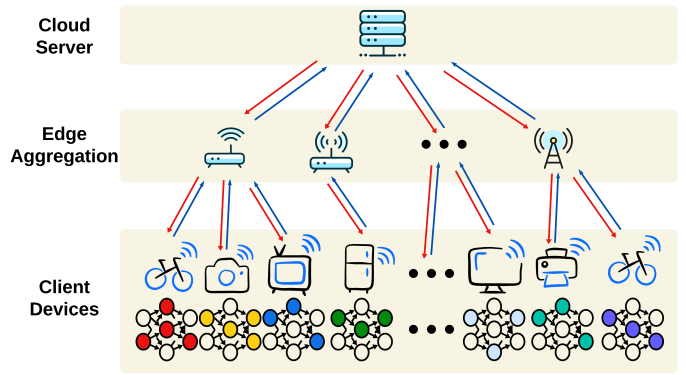


Fig. 1: H-FedSN: Personalized and structured sparse models for each client to achieve high communication efficiency while maintaining model accuracy within the HFL architecture for realistic IoT environment.

compared to the traditional HFL method HierFAVG in our experiments. It achieves this by transmitting only a binary mask (1 bit per element) instead of full model weights (32 bits per element), and by excluding personalized layers from edge and cloud aggregation. To further enhance model accuracy and address imbalanced client distribution, H-FedSN incorporates Bayesian aggregation at both edge and cloud levels. This method uses cumulative updates of Beta distribution parameters to balance contributions from edge nodes with varying numbers of connected clients. While edge nodes with more clients have a larger immediate impact on parameter updates, the cumulative nature of these updates ensures a fair representation of all edge nodes over time. Combined with the locally retained personalized mask layers, this approach allows the system to adapt to imbalanced client distributions across edges and achieve high model accuracy.

We conduct our experiments on three real-world IoT datasets (WISDM (WATCH) [19], WIDAR [20], [21], and WISDM (PHONE) [22] datasets) and the MNIST [23] dataset under Non-IID data setting [24]. We compare our H-FedSN with HierFAVG, a traditional HFL method, and two types of FL methods: (1) Personalization for enhancing model accuracy (FedPer [18] and FedRS [17]); (2) Communication reduction (FedCAMS [16] and TOPK [25] 32x parameter compression) within the three-tier HFL architecture. The experimental results demonstrated that the communication cost of H-FedSN was significantly lower than all baseline methods, reducing it by at least 58 times compared to HierFAVG (approximately 238 times on the MNIST dataset and about 136 times on the WIDAR dataset). Regarding accuracy, H-FedSN achieves much better results by an average of 8.6% compared to communication-enhanced FL methods and is comparable to personalized FL methods within HFL architecture.

II. RELATED WORK

A. Federated Learning and Its Limitations in Real-World IoT Scenarios

FL has revolutionized distributed machine learning by enabling collaborative model training across multiple clients without centralizing data, enhancing privacy and security. Pioneering algorithms such as FedAvg [4], FedProx [5], and Scaffold [6] have demonstrated effective collaborative training across diverse nodes. However, traditional FL approaches face significant challenges in real-world Internet of Things (IoT) scenarios, primarily due to their two-tier architecture being incompatible with the inherent multi-tier structure of IoT environments. As mentioned in the introduction, smart city surveillance and agricultural IoT systems naturally form three-tier structures. Similarly, in industrial IoT settings, a three-tier structure emerges with factory floor devices as clients, local servers as edge nodes, and a central manufacturing system as the cloud for global aggregation [26]. Another example of a three-tier IoT architecture can be found in smart healthcare systems for remote patient monitoring [27]. In this scenario, wearable devices and home health monitors at the client layer collect patient data and run basic health models. At the edge layer, local healthcare facilities' servers aggregate data from multiple patients. The cloud layer, typically a central hospital or health system cloud server, performs global aggregation across all patients and facilities. This multi-tier structure allows for efficient data processing and model training at different levels of granularity, from individual patient monitoring to population-level health trend analysis.

These examples illustrate that real-world IoT applications inherently operate within a three-tier or multi-tier architecture, which traditional two-tier FL algorithms are not designed to accommodate efficiently. Additionally, as the number of IoT devices grows, traditional FL architectures face scalability issues, potentially leading to processing delays and central server overload [28].

B. Communication Efficiency and Accuracy Challenges in Federated Learning and HFL

In traditional FL, researchers have developed various approaches to address challenges of communication efficiency and model accuracy. For communication efficiency, methods like FedAvg [4] reduce communication rounds through multiple local updates before aggregation. More advanced techniques include FedSCR [29], which reduces upstream communication through structure-based methods, and approaches that balance communication-computation trade-offs [30] or employ network pruning [31]. To improve model accuracy, especially in non-IID settings, algorithms such as FedProx [5] introduce proximal terms to stabilize training, while Scaffold [6] uses control variates to correct for client drift. Personalized FL methods [14], [18] have also been proposed to handle heterogeneous data distributions across clients.

However, these solutions, while effective in traditional FL settings, are not directly applicable to Hierarchical Federated

Learning (HFL) scenarios, particularly in IoT environments. HFL's multi-tier architecture, typically consisting of client, edge, and cloud layers, introduces new complexities. In HFL, model updates must traverse multiple levels, increasing overall latency and bandwidth consumption. Traditional FL communication reduction techniques are not designed to address this multi-level structure, and research on adapting these techniques to HFL scenarios is lacking [32]. Moreover, HFL can exacerbate issues related to non-IID data, as heterogeneity exists not only among clients but also across different hierarchy levels. This multi-level heterogeneity, combined with the uneven distribution of devices across edge servers in real-world IoT scenarios, can lead to more severe model divergence and accuracy degradation compared to traditional FL settings [33], [34]. Existing accuracy improvement methods for FL often assume a flat structure and can not directly address these cascading effects of data and device heterogeneity in a hierarchical setting.

These issues highlight the need for novel solutions designed for HFL in IoT environments. Our proposed algorithm, H-FedSN, significantly enhances communication efficiency by transmitting only binary masks between clients, edge nodes, and the cloud. Each client trains a model comprising both shared and private layers, with the private layers specifically designed to capture individualized data characteristics, thus improving accuracy. Furthermore, H-FedSN employs Bayesian aggregation for more efficient model updates across the hierarchical structure, effectively balancing contributions from diverse client groups and addressing the challenges of non-IID data and imbalanced device distribution in HFL scenarios.

III. H-FEDSN DESIGN

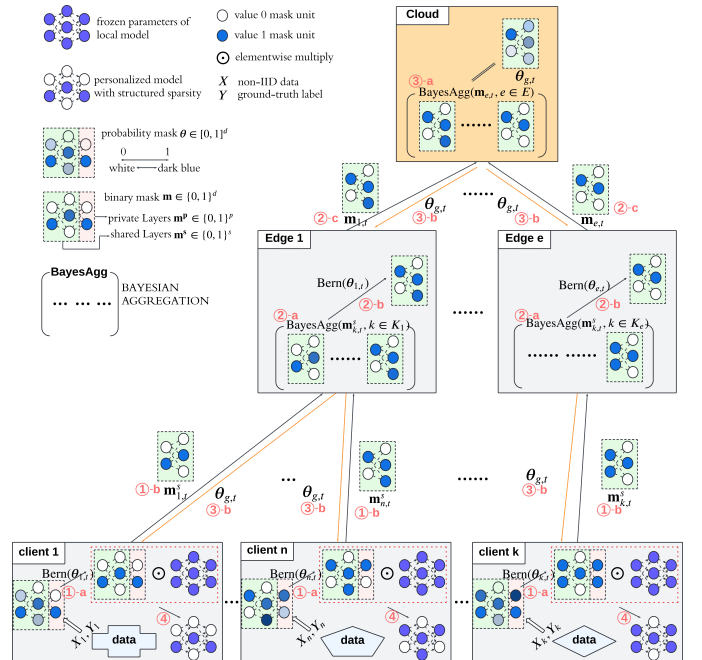


Fig. 2: Overview of H-FedSN framework.

A. Overview

H-FedSN is an algorithm based on the HFL architecture, designed to optimize communication efficiency and ensure model accuracy through efficient mask training, personalized layers, and Bayesian aggregation. Zhou et al. demonstrated that training sparse models with masks, while keeping the model parameters unchanged, is an effective alternative to traditional training methods [35].

Fig. 2 depicts an overview of the proposed H-FedSN framework. H-FedSN allows each client to freeze its randomly initialized local model parameters $\mathbf{w}_{\text{init}} = (w_{\text{init}}^1, w_{\text{init}}^2, \dots, w_{\text{init}}^d) \in \mathbb{R}^d$ while collaboratively training a personalized probability mask $\boldsymbol{\theta}_k \in [0, 1]^d$ for each client k , using their respective local datasets D_k . This probability mask $\boldsymbol{\theta}_k$ determines the activation probability of the local model parameters and serves as the Bernoulli parameter for the stochastic binary mask $\mathbf{m}_k \sim \text{Bern}(\boldsymbol{\theta}_k) \in \{0, 1\}^d$ (1-a). The binary mask \mathbf{m}_k is then applied to the frozen parameters \mathbf{w}_{init} to create a structured sparse model, uniquely personalized for each client (4). The resulting model, expressed as $\hat{w}_k = \mathbf{m}_k \odot \mathbf{w}_{\text{init}}$, is optimized to enhance performance on specific tasks. For a more detailed description of the algorithm, please refer to Algorithm 1.

At the client level, each client k is associated with an edge server e and is part of the set K_e . Here, e represents a specific edge server, and K_e denotes the set of all clients connected to that particular edge server e . This setup implies multiple edge servers, each managing its own group of clients. Clients are responsible for training a probability mask $\boldsymbol{\theta}_k$, which is dimensioned $[0, 1]^d$ to match the size of the client's local model parameters. Especially, the probability mask is bifurcated into a shared layer $\boldsymbol{\theta}_k^s \in [0, 1]^s$ and a private layer $\boldsymbol{\theta}_k^p \in [0, 1]^p$. The shared layer's parameters, meant for aggregation, enhance the model by leveraging collective insights, while the private layer's parameters are tailored for local data specificity and privacy, hence not shared. Based on this probability mask, the binary mask $\mathbf{m}_k = \text{Bern}(\boldsymbol{\theta}_k)$ inherits the bifurcated structure of $\boldsymbol{\theta}_k$, comprising shared \mathbf{m}_k^s and private \mathbf{m}_k^p layers. This structured approach ensures that while personalization is maintained through private layers, the collaborative benefits of federated learning are realized by the shared layers.

Each edge server e , where $e \in E$, is responsible for collecting binary masks \mathbf{m}_k^s , $k \in K_e$ (1-b). These edge servers aggregate (2-a) the masks using a Bayesian aggregation method, which allows adaptation to various data distributions and improves performance through refined model updates. Post-aggregation, the edge server computes a consolidated probability mask $\boldsymbol{\theta}_e \in [0, 1]^s$ from the aggregated data and uses it to generate binary masks $\mathbf{m}_e \in \{0, 1\}^s$ through a Bernoulli sampling process (2-b), which are then sent to the cloud server for further processing (2-c).

The cloud server plays a pivotal role in integrating the updates received from various edge servers. It performs the final aggregation of the binary masks \mathbf{m}_e uploaded by the edge

Algorithm 1 H-FedSN

Require: Number of training rounds T , number of local iterations τ , learning rate η , initial Beta distribution parameters $\lambda_0 = 1$

Ensure: Training a personalized and structured sparse model unique to each client.

- 1: At the cloud server, initialize Beta priors $\alpha_g^0 = \beta_g^0 = \lambda_0$, and initialize a random network with weight vector $\mathbf{w}_{\text{init}} \in \mathbb{R}^d$, and then broadcast it to the clients through edges.
 - 2: At the edge servers, initialize Beta priors $\alpha_e^0 = \beta_e^0 = \lambda_0$.
 - 3: For all clients, initialize random mask probability $s_{k,1}$
 - 4: **for** $t = 1$ to T **do**
 - 5: **for** each edge server $e \in E$ **in parallel do**
 - 6: **Edge server:**
 - 7: **for** each client $k \in K_e$ **in parallel do**
 - 8: **Client:**
 - 9: **if** $t > 1$ **then**
 - 10: $\boldsymbol{\theta}_{k,t} \leftarrow \boldsymbol{\theta}_{g,t-1} + \boldsymbol{\theta}_{k,t-1}^p$
 - 11: $s_{k,t} \leftarrow \text{Sigmoid}^{-1}(\boldsymbol{\theta}_{k,t})$
 - 12: **end if**
 - 13: **for** $i = 1$ to τ **do**
 - 14: $\boldsymbol{\theta}_{k,t} \leftarrow \text{Sigmoid}(s_{k,t})$
 - 15: $\mathbf{m}_{k,t} \leftarrow \text{Bern}(\boldsymbol{\theta}_{k,t})$
 - 16: $\hat{w}_{k,t} \leftarrow \mathbf{m}_{k,t} \odot \mathbf{w}_{\text{init}}$
 - 17: Compute loss $L(f(\hat{w}_{k,t}), D_k)$
 - 18: $s_{k,t} \leftarrow s_{k,t} - \eta \nabla L(f(\hat{w}_{k,t}), D_k)$
 - 19: **end for**
 - 20: $\boldsymbol{\theta}_{k,t} \leftarrow \text{Sigmoid}(s_{k,t})$
 - 21: $\mathbf{m}_{k,t} \leftarrow \text{Bern}(\boldsymbol{\theta}_{k,t})$
 - 22: Upload $\mathbf{m}_{k,t}^s$ to edge server e
 - 23: **end for**
 - 24: **Edge server:**
 - 25: $\mathbf{m}_{e,t} = \text{BayesianAggregationAtEdge}(\{\mathbf{m}_{k,t}^s\}_{k \in K_e}, t)$
 - 26: Upload $\mathbf{m}_{e,t}$ to cloud server
 - 27: **end for**
 - 28: **Cloud server:**
 - 29: $\boldsymbol{\theta}_{g,t} = \text{BayesianAggregationAtCloud}(\{\mathbf{m}_{e,t}\}_{e \in E}, t)$
 - 30: Broadcast $\boldsymbol{\theta}_{g,t}$ to all edges $e \in E$, and all clients
 - 31: **end for**
 - 32: For all clients, $\mathbf{m}_{k,\text{final}} = \text{Bern}(\boldsymbol{\theta}_{g,T} + \boldsymbol{\theta}_{k,T}^p)$. Generate the final model: $\hat{w}_{k,\text{final}} \leftarrow \mathbf{m}_{k,\text{final}} \odot \mathbf{w}_{\text{init}}$.
-

servers to form a global probability mask $\boldsymbol{\theta}_g \in [0, 1]^s$ (3-a). This global mask $\boldsymbol{\theta}_g$ is then broadcast back to all clients through the edge servers (3-b), facilitating a synchronized update across the network. This mechanism ensures that the global model is continually refined and updated based on the collective learning from all participating clients.

B. Local Training in Client

In H-FedSN, for round t , clients initially receive a global shared probability mask $\boldsymbol{\theta}_{g,t-1}$ from the cloud server. Clients combine $\boldsymbol{\theta}_{g,t-1}$ with $\boldsymbol{\theta}_{k,t-1}^p$ to generate $\boldsymbol{\theta}_{k,t} \in [0, 1]^d$, which represents the activation probabilities of the model parameters. To optimize within a broader parameter space, this probability

mask is transformed into a *score mask* $\mathbf{s} = (s^1, s^2, \dots, s^d) \in \mathbb{R}^d$ via the inverse Sigmoid function. This transformation allows the *score mask* \mathbf{s} to vary freely within the real number range, providing more flexibility for subsequent optimization. This design permits the *score mask* to flexibly generate the corresponding probability mask by setting $\boldsymbol{\theta} = \text{Sigmoid}(\mathbf{s})$, ensuring each value is appropriately within the $[0, 1]$ interval. The detailed steps for local probability mask training in round t are described as follows and can also be seen in Algorithm 1 (lines 8-21):

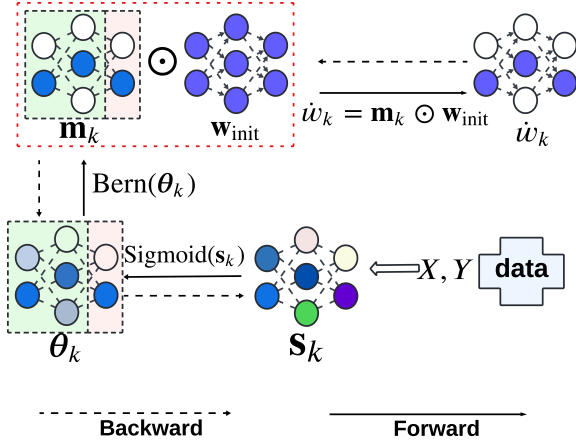


Fig. 3: H-FedSN Local Training in Client.

- 1) Clients receive the global probability mask $\boldsymbol{\theta}_{g,t-1}$ from the cloud server, then combine $\boldsymbol{\theta}_{g,t-1}$ with $\boldsymbol{\theta}_{k,t-1}^p$ to generate $\boldsymbol{\theta}_{k,t}$. Each client then inputs this probability mask into the inverse Sigmoid function $\text{Sigmoid}^{-1}(\cdot)$, obtaining the *score mask* $\mathbf{s}_{k,t} = \text{Sigmoid}^{-1}(\boldsymbol{\theta}_{k,t})$.
- 2) Clients transform back to $\boldsymbol{\theta}_{k,t} = \text{Sigmoid}(\mathbf{s}_{k,t})$, then use Bernoulli sampling to extract binary masks $\mathbf{m}_{k,t}$ from $\boldsymbol{\theta}_{k,t}$.
- 3) The sampled binary mask $\mathbf{m}_{k,t}$ is used to sparsify the initial weight vector \mathbf{w}_{init} : $\hat{\mathbf{w}}_{k,t} = \mathbf{m}_{k,t} \odot \mathbf{w}_{\text{init}}$.
- 4) The $\hat{\mathbf{w}}_{k,t}$ is utilized for forward propagation to compute the outputs, and the computed local loss $L(f(\hat{\mathbf{w}}_{k,t}), D_k)$ is then used in backpropagation to update the *score mask* according to the formula $\mathbf{s}_{k,t} = \mathbf{s}_{k,t} - \eta \nabla L(f(\hat{\mathbf{w}}_{k,t}), D_k)$ (where η is the local learning rate).

Fig. 3 illustrates the process of a single epoch of local training on a client. Steps 2 to 4 involve all local operations that are differentiable, except for the Bernoulli sampling step. Since Bernoulli sampling itself is non-differentiable, this would pose a problem in traditional gradient descent frameworks. To address this, we adopt the straight-through estimator technique proposed by [36]. This technique allows us to "pass-through" gradients during the Bernoulli sampling process: during backpropagation, we set the output gradient of the Bernoulli function to be equal to the input probability mask $\boldsymbol{\theta}_{k,t}$. Thus, although the sampling step is not differentiable, we can still effectively propagate gradients throughout the network and update the score mask $\mathbf{s}_{k,t}$.

After τ training rounds, each client completes the training of their local probability mask $\boldsymbol{\theta}_{k,t} = \text{Sigmoid}(\mathbf{s}_{k,t})$ and generates a binary mask $\mathbf{m}_{k,t} = \text{Bern}(\boldsymbol{\theta}_{k,t})$ through Bernoulli sampling. The client keeps the private part, $\mathbf{m}_{k,t}^p$, and uploads the shared layers, $\mathbf{m}_{k,t}^s$, to the respective connected edge server. The next step involves the edge server aggregating these binary masks to form a comprehensive model update.

C. Bayesian Aggregation in HFL

In the HFL architecture, both edge and cloud servers implement a Bayesian aggregation strategy to process the binary masks they receive. This approach marks a significant departure from traditional federated learning methods, such as FedAvg, which primarily rely on simple averaging to aggregate updates. Unlike these conventional methods, H-FedSN leverages Bayesian aggregation to more effectively account for the inherent uncertainties in data updates. This capability allows H-FedSN to construct more robust and adaptive global models by synthesizing updates represented as binary masks from clients across multiple layers of the architecture.

The subsequent sections provide a detailed description of the aggregation processes at both the edge server and cloud server levels.

1) Edge Server Bayesian Aggregation:

As shown in Fig. 4, each edge server e , $e \in E$, is responsible for collecting binary masks $\mathbf{m}_{k,t}^s$ uploaded by all directly connected clients k , $k \in K_e$, at round t . The edge server employs a Bayesian aggregation method, as shown in Algorithm 2, to integrate these binary masks into an edge probability mask $\boldsymbol{\theta}_{e,t}$. Specifically, the probability mask $\boldsymbol{\theta}_{e,t}$ is modeled using the parameters of a Beta distribution, $\alpha_{e,t}$ and $\beta_{e,t}$, which are initially set to $\alpha_{e,0} = \beta_{e,0} = \lambda_0$.

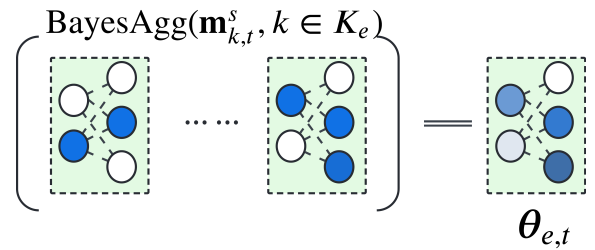


Fig. 4: Edge Server Bayesian Aggregation At Round t .

At the start of training, lacking any prior knowledge about which network weights are more important, each value in the probability mask is uniformly distributed between $[0, 1]$, forming the prior distribution. Based on the client's local binary masks $\mathbf{m}_{k,t}^s$ from client k , the edge server updates its beliefs about the importance of weights, forming a new posterior distribution. Due to the conjugate relationship between Beta and Bernoulli distributions, the updated posterior remains a

Beta distribution, with parameters updated as follows:

$$\begin{aligned}\alpha_{e,t} &= \alpha_{e,t-1} + \sum_{k \in K_e} \mathbf{m}_{k,t}^s \\ \beta_{e,t} &= \beta_{e,t-1} + |K_e| \cdot \mathbf{1} - \sum_{k \in K_e} \mathbf{m}_{k,t}^s\end{aligned}$$

Here, $\mathbf{m}_{k,t}^s$ represents the binary mask submitted by the k -th client under edge server e during round t . The $\mathbf{1}$ is the s -dimensional all-ones vector. $|K_e|$ denotes the number of clients connected to edge server e .

Subsequently, the edge server calculates the probability mask $\theta_{e,t}$ based on the updated parameters $\alpha_{e,t}$ and $\beta_{e,t}$:

$$\theta_{e,t} = \frac{\alpha_{e,t} - 1}{\alpha_{e,t} + \beta_{e,t} - 2}$$

This operation is applied element-wise. The edge server then broadcasts $\mathbf{m}_{e,t} = \text{Bern}(\theta_{e,t})$ to the cloud. To avoid model overfitting to historical data, $\alpha_{e,t}$ and $\beta_{e,t}$ should be reset to their initial value $\lambda_0 = 1$ at the start of every 10^{th} training round.

Algorithm 2 Bayesian Aggregation At Edge

Require: Binary masks $\mathbf{m}_{k,t}^s$ from clients $k \in K_e$, and round number t

Ensure: Updated binary mask $\mathbf{m}_{e,t}$

- 1: **if** ResPriors(t) **then**
 - 2: $\alpha_{e,t-1} = \beta_{e,t-1} = \lambda_0$
 - 3: **end if**
 - 4: $\alpha_{e,t} = \alpha_{e,t-1} + \sum_{k \in K_e} \mathbf{m}_{k,t}^s$
 - 5: $\beta_{e,t} = \beta_{e,t-1} + |K_e| \cdot \mathbf{1} - \sum_{k \in K_e} \mathbf{m}_{k,t}^s$
 - 6: $\theta_{e,t} = \frac{\alpha_{e,t} - 1}{\alpha_{e,t} + \beta_{e,t} - 2}$
 - 7: $\mathbf{m}_{e,t} \leftarrow \text{Bern}(\theta_{e,t})$
 - 8: **Output:** $\mathbf{m}_{e,t}$
-

2) Cloud Server Bayesian Aggregation:

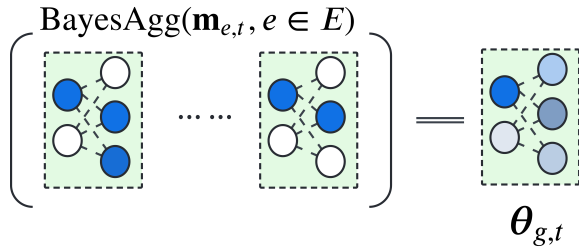


Fig. 5: Cloud Server Bayesian Aggregation At Round t .

The cloud server is responsible for collecting the binary masks uploaded by all edge servers e , $e \in E$, and performs a global aggregation once all uploads are complete to generate a global probability mask. At the cloud level, as illustrated in Fig. 5 and Algorithm 3, the global probability mask $\theta_{g,t}$ is modeled using a Beta distribution $\text{Beta}(\alpha_{g,t}, \beta_{g,t})$, with parameters $\alpha_{g,t}$ and $\beta_{g,t}$ related to the training round and

initially set to $\alpha_{g,0} = \beta_{g,0} = \lambda_0$. The parameters for the updated posterior distribution are calculated as follows:

$$\begin{aligned}\alpha_{g,t} &= \alpha_{g,t-1} + \sum_{e \in E} \mathbf{m}_{e,t} \\ \beta_{g,t} &= \beta_{g,t-1} + |E| \cdot \mathbf{1} - \sum_{e \in E} \mathbf{m}_{e,t}\end{aligned}$$

Here, $\mathbf{m}_{e,t}$ represents the binary mask submitted by the e -th edge server to the cloud during round t . The $\mathbf{1}$ is the s -dimensional all-ones vector. $|E|$ denotes the number of edge servers. Following the parameter update, the cloud server computes the mode of the Bernoulli distributions to derive the global probability mask $\theta_{g,t}$, as suggested by [37]:

$$\theta_{g,t} = \frac{\alpha_{g,t} - 1}{\alpha_{g,t} + \beta_{g,t} - 2}$$

Subsequently, the cloud broadcasts the probability mask $\theta_{g,t}$ to all clients through the edge servers. To avoid model overfitting to historical data, $\alpha_{g,t}$, and $\beta_{g,t}$ should be reset to their initial value $\lambda_0 = 1$ at the start of every 10^{th} training round.

Algorithm 3 Bayesian Aggregation At Cloud

Require: Binary masks $\mathbf{m}_{e,t}$ from edge servers $e \in E$, and round number t

Ensure: Updated global probability mask $\theta_{g,t}$

- 1: **if** ResPriors(t) **then**
 - 2: $\alpha_{e,t-1} = \beta_{e,t-1} = \lambda_0$
 - 3: **end if**
 - 4: $\alpha_{g,t} = \alpha_{g,t-1} + \sum_{e \in E} \mathbf{m}_{e,t}$
 - 5: $\beta_{g,t} = \beta_{g,t-1} + |E| \cdot \mathbf{1} - \sum_{e \in E} \mathbf{m}_{e,t}$
 - 6: $\theta_{g,t} = \frac{\alpha_{g,t} - 1}{\alpha_{g,t} + \beta_{g,t} - 2}$
 - 7: **Output:** $\theta_{g,t}$
-

IV. EXPERIMENTS

In this section, we empirically evaluate the performance of H-FedSN, focusing on both accuracy and communication costs. Our experimental analysis covers four distinct datasets: the widely-utilized MNIST [23], supplemented by three IoT-specific datasets: WISDM (watch) [19], WIDAR [20], [21], and WISDM (phone) [22]. MNIST acts as a general benchmark, while the inclusion of IoT datasets showcases our method's applicability in real-world IoT settings. We conduct a comparative analysis of H-FedSN against 5 established baselines within the HFL architecture. Notably, while HierFAVG [9] are native to the HFL architecture, the other baselines—FedPer [18], FedRS [17], FedCAMS [16], and TOPK [25]—originally designed for the standard FL architecture, have been adapted for HFL architecture to ensure a consistent evaluation framework.

A. Datasets Setting

1) *Datasets and Preprocessing:* Table I shows the statistical distribution of the datasets used in our experiments. Below, we describe each dataset along with its preprocessing methods:

TABLE I: Statistical information of datasets.

Dataset	Dimension	# Samples (Train / Test)	Classes	#Fixed Classes per Client
MNIST	28 x 28	500,000 / 10,000	10	6
WISDM (WATCH)	200 x 6	16,569 / 4,103	12	7
WIDAR	22 x 20 x 20	11,372 / 5,222	9	5
WISDM (PHONE)	200 x 6	13,714 / 4,073	12	7

- **MNIST** comprises handwritten digits across 10 classes, widely used for image classification model training [23]. Preprocessing involved converting images to tensors and normalizing pixel values to $[-1, 1]$.
- **WISDM (WATCH)** [19] encompasses accelerometer and gyroscope readings from smartwatches, capturing 18 daily activities performed by 51 participants. Our preprocessing approach aligned with established methods in the field of sensor-based activity recognition [38], [39], [40]. We segmented each 3-minute recording using a sliding window technique, employing a 10-second window with 50% overlap. Subsequently, we applied normalization to each dimension of the resulting samples, centering the data around zero and adjusting the scale to achieve unit variance.
- **WIDAR** [20], [21], designed for contactless gesture recognition using Wi-Fi signal strength, includes data from 17 participants performing 22 unique gestures. We applied body velocity profiling (BVP) to account for environmental variations, followed by scalar normalization. The final representation was structured into $22 \times 20 \times 20$ samples, covering the time axis and x-y velocity features. Only gestures recorded by more than three users were retained to ensure consistency between training and testing sets.
- **WISDM (PHONE)** [22] consists of accelerometer data obtained from smartphones during participants’ daily activities. We implemented an identical preprocessing protocol to that used for the WISDM (WATCH) dataset. This involved segmenting the data with a 10-second sliding window (50% overlap), followed by normalization of each dimension to zero mean and unit variance.

2) *Data Partitioning and Non-IID Setting*: To simulate non-IID data distributions, we implemented the Quantity-based Label Imbalance method. This approach ensures that each participant, or client, owns data samples of a fixed number of labels, a strategy initially introduced in the experiments of FedAvg [4]. Enhancing this methodology, we adopted the general partitioning strategy introduced by Li et al., [24]. This strategy meticulously sets the number of labels that each party has, ensuring that each participant only has data samples of n different labels. We begin by randomly assigning n different label IDs to each party. Then, we distribute the samples of each label randomly and equally among the parties that own these labels. This approach guarantees that the number of labels in each party is fixed and there is no overlap of samples between different parties, fostering a truly non-IID data environment. Importantly, to ensure the consistency of our experimental conditions, the distribution patterns for both training and test datasets are identical, maintaining the same level of label imbalance across all data divisions. Table I

displays the total number of classes in various datasets along with the fixed number of classes each client has. Furthermore, for a more intuitive understanding of the data distribution under this method, Fig. 6 shows the distribution of the WIDAR dataset across 5 clients as an example.

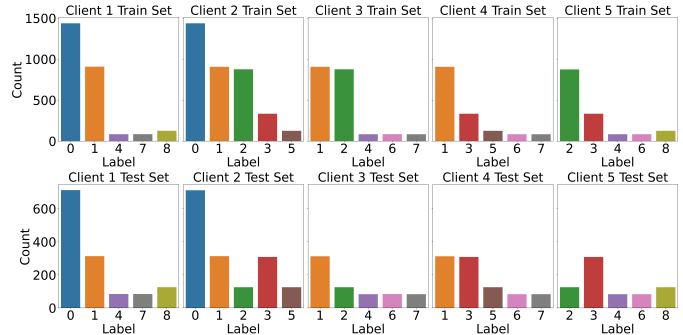


Fig. 6: WIDAR Dataset NoN-IID Data Distribution Across 5 Clients

B. Experimental Design

1) H-FedSN and Baselines Setting:

H-FedSN. We used a 4-layer convolutional neural network (CNN) comprising two convolutional blocks (each with two convolutional layers followed by a pooling layer, with 64 filters per layer in the first block and 128 in the second) and three fully-connected layers (two with 256 units each, followed by an output layer matching the dataset’s number of classes). For H-FedSN, we set the last three layers as private layers, which do not participate in the aggregation process.

To comprehensively evaluate the performance of H-FedSN, we compare H-FedSN against 5 baselines:

- **HierFAVG** [9] Hierarchical federated averaging with client-edge-cloud structure.
- **FedPer** [18] Federated personalization keeping part of model parameters local.
- **FedRS** [17] Addresses label distribution skew using Restricted Softmax.
- **FedCAMS** [16] Combines gradient compression with adaptive optimization to reduce communication overhead.
- **TOPK** [25] Sparsification method selecting largest k (3.125%) elements of gradients.

All baselines are implemented with aggregations at both edge and cloud levels in the HFL architecture.

In addition, we adopted the same base model configuration for each baseline method, which is the same 4-layer CNN (CONV-4) used for H-FedSN. We also applied the same data configurations, ensuring consistency across all experiments with the non-IID data distribution.

2) *Performance Metrics*: To comprehensively assess the efficacy of our proposed algorithm, we evaluate the following key performance metrics:

- **Inference Performance:** We evaluated the inference accuracy of our algorithm by analyzing it on each device’s test data. We then reported the distribution of accuracies across

all devices, providing insights into the algorithm’s ability to handle data heterogeneity and the overall model’s inference accuracy distribution trend, even under conditions of device imbalance.

- **Communication Overhead:** We assessed the volume of data transmitted during the training process between clients and edge servers, as well as from edge servers to the cloud. This metric is crucial in IoT scenarios where bandwidth is often limited. Reducing communication volume is essential for enhancing network performance, minimizing congestion, and improving the scalability of the system.

3) *Experimental Setting:* To illustrate the adaptability of our proposed algorithm across different scenarios and environments, we designed the following experimental configurations:

- **E2C5:** 2 edge nodes and 5 client nodes. This minimalistic setup tests the algorithm’s effectiveness in small-scale deployments, such as some small offices or local retail stores with limited devices and minimal infrastructure [41].
- **E20C50:** 20 edge nodes and 50 client nodes. This configuration evaluates scalability and robustness in larger, complex network topologies, simulating environments like a smart city surveillance system across multiple buildings [7].
- **E2C50:** 2 edge nodes and 50 client nodes. This setting simulates high client density scenarios, such as a smart healthcare system for remote patient monitoring where numerous wearable devices and home health monitors connect to local healthcare facility servers [27].
- **Imbalanced E5C50:** 5 edge nodes with 50 clients distributed in ratios of 0.4, 0.2, 0.2, 0.1, and 0.1. This imbalanced setup tests consistency and fairness across unevenly distributed network nodes, representing scenarios like smart agriculture systems with varying device densities across different farm sections [8].

For all experiments, the hyperparameters were consistently set as follows: Global Rounds = 200, Epochs per Round = 20, and Batch Size = 128. The learning rates for H-FedSN were 0.01 for all datasets except the WIDAR dataset, where the learning rate was 0.035. For the baseline algorithms, the learning rate was uniformly set to 0.001.

C. Results and Analysis

In this section, we present and analyze the results obtained from our experiments. We provide a comparative evaluation of H-FedSN against the baselines in terms of inference performance and communication costs.

1) E2C5 Configuration:

In the **E2C5** configuration (Fig. 7), H-FedSN achieves the lowest communication cost among all baseline methods. For the MNIST dataset, H-FedSN reduces communication by approximately 238.8 times compared to HierFAVG, from 60414.31 KB to 252.94 KB. This substantial reduction is achieved through the use of masking techniques that effectively compress data during transfer and the retention of personalized layers that are not transmitted and aggregated, further reducing communication costs. Despite this significant reduction in communication overhead, H-FedSN maintains

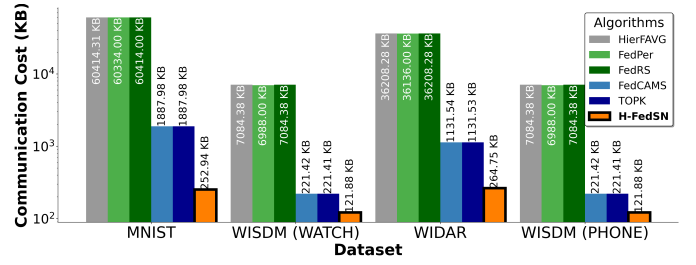


Fig. 7: Communication cost for different algorithms across different datasets in **E2C5** configuration.

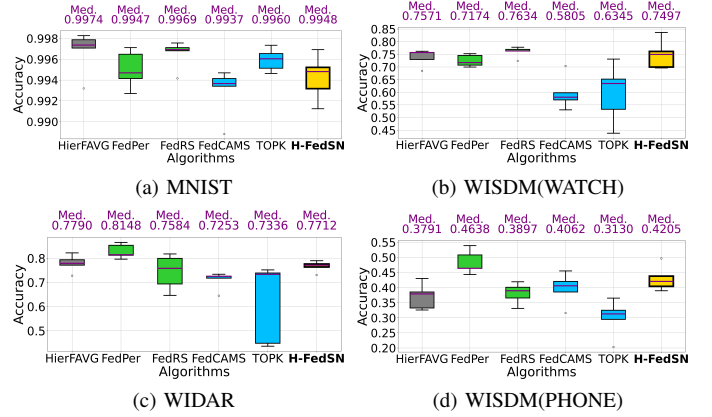


Fig. 8: Inference accuracy for different algorithms across different datasets in **E2C5** configuration.

comparable precision, with an accuracy deviation for the MNIST dataset of only 0.26%, as shown in Fig. 8. For the IoT datasets (WISDM watch, WIDAR, and WISDM phone), H-FedSN also shows comparable accuracy while significantly reducing communication costs. H-FedSN achieves such high accuracy due to the use of personalized layers and Bayesian aggregation techniques. These techniques enhance the H-FedSN to handle heterogeneous data, thus achieving a balance of high accuracy and low communication cost.

2) E20C50 Configuration:

In the **E20C50** configuration, H-FedSN maintains minimal communication costs while achieving comparable inference accuracy to baseline methods across all datasets. As detailed in Fig. 9, H-FedSN significantly reduces communication expenses when compared to the baseline methods. Despite the larger scale of the network, H-FedSN efficiently compresses data through masking techniques, reducing the amount of data transmitted without compromising performance. Fig. 10 shows that the inference accuracy for H-FedSN is comparable to, if not better than, the baseline methods, demonstrating robustness and scalability.

3) E2C50 Configuration:

The **E2C50** configuration, where each edge node handles a high density of clients, demands efficient management of substantial data exchanges and communication requirements. As shown in Fig. 11, the H-FedSN method transmits the small-

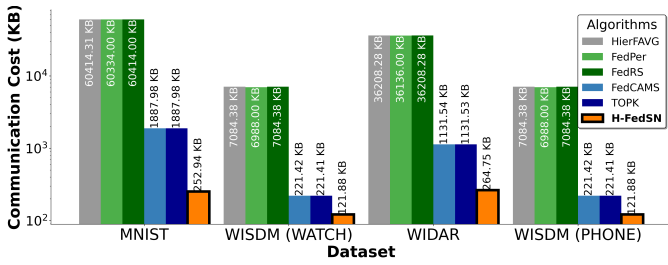


Fig. 9: Communication cost for different algorithms across different datasets in **E2C50** configuration.

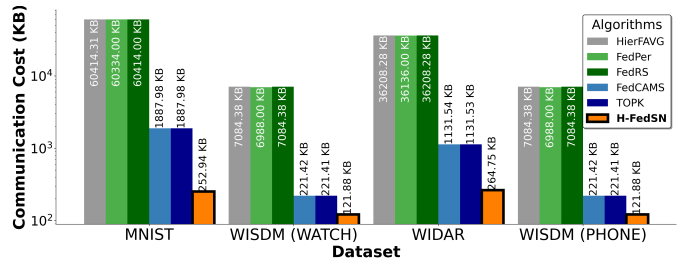


Fig. 11: Communication cost for different algorithms across different datasets in **E2C50** configuration.

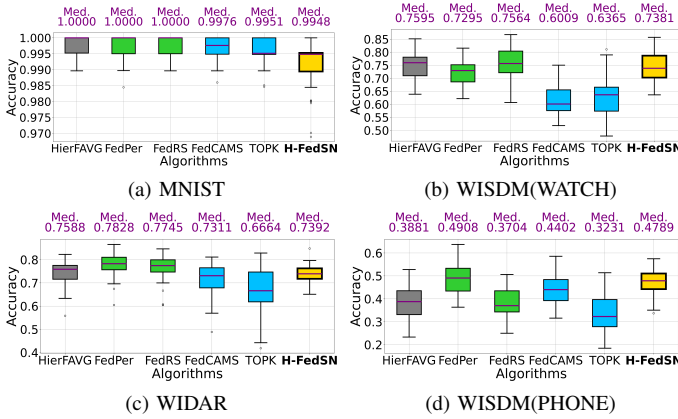


Fig. 10: Inference accuracy for different algorithms across different datasets in **E2C50** configuration.

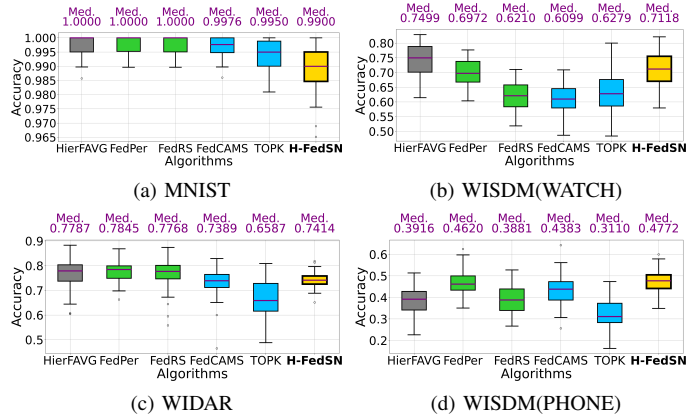


Fig. 12: Inference accuracy for different algorithms across different datasets in **E2C50** configuration.

est volume of model parameters compared to other baselines, resulting in the lowest communication costs. Despite the high-density client environment at each edge, H-FedSN achieves a significant reduction in communication overhead while maintaining comparable inference accuracy, as illustrated in Fig. 12.

4) Imbalanced E5C50 Configuration:

In the **Imbalanced E5C50** configuration, where client distribution is uneven, H-FedSN demonstrates its robustness by maintaining high performance across varying client densities while significantly reducing communication costs across all datasets. As shown in Fig. 13 and Fig. 14, the algorithm achieves accuracy levels comparable to baseline methods while simultaneously minimizing communication overhead. This consistent performance is attributed to the strategic use of personalized layers and Bayesian aggregation, which effectively address heterogeneity and imbalance. By employing personalized layers and efficient masking techniques, the amount of model parameters exchanged between clients is significantly reduced, leading to the lowest communication costs among all evaluated methods. This ability to minimize communication overhead while preserving high accuracy highlights H-FedSN's advantages in addressing the challenges of device/data imbalance and communication efficiency in real-world distributed learning environments.

In summary, H-FedSN demonstrates a significant reduction in communication costs while maintaining or even improving

inference accuracy compared to baseline methods. In comparison to other personalization methods adapted for hierarchical federated learning, such as FedPer and FedRS, H-FedSN maintains comparable accuracy but achieves significantly lower communication costs. Additionally, H-FedSN outperforms communication-efficient methods like FedCAMS and TOPK, which were originally designed to reduce communication in standard federated learning. H-FedSN reduces communication costs further while achieving higher accuracy, highlighting its superior efficiency and performance in hierarchical federated learning environments.

V. CONCLUSION

In this paper, we propose H-FedSN, a novel method to address the challenges of model accuracy and communication efficiency faced by HFL in IoT environments. H-FedSN trains a sparse network within each client in the HFL setting. Our experiments demonstrate that H-FedSN significantly outperforms baselines in reducing communication costs while maintaining or improving inference accuracy. The key innovations, including masking techniques for effective data transfer, local retention of personalized layers, and Bayesian aggregation at edge and cloud levels, ensure robustness and efficiency in the face of data heterogeneity, imbalanced device distribution, and limited communication resources, which are common in real-world IoT applications. As a result, H-FedSN not only

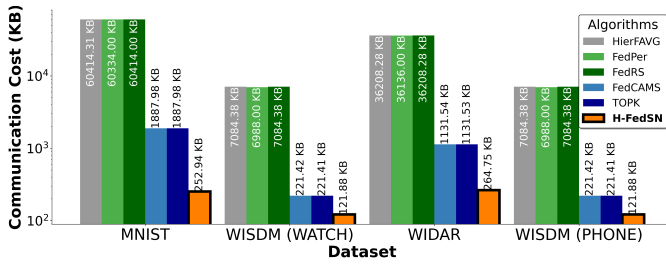


Fig. 13: Communication cost for different algorithms across different datasets in **Imbalanced E5C50** configuration.

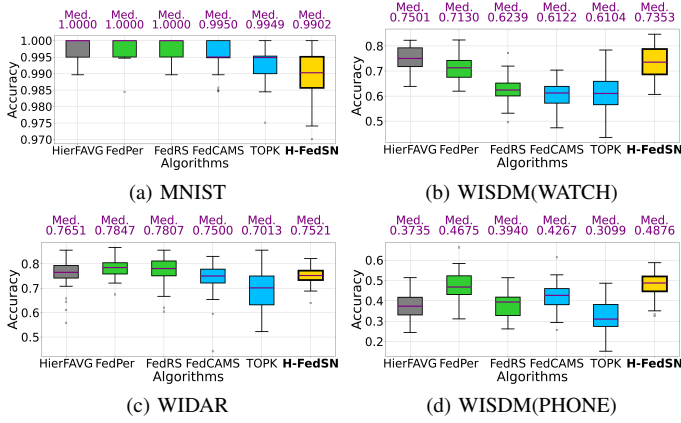


Fig. 14: Inference accuracy for different algorithms across different datasets in **Imbalanced E5C50** configuration.

presents a promising solution for enabling efficient and accurate hierarchical federated learning in resource-constrained IoT environments but also offers insights for other distributed learning scenarios with similar challenges.

REFERENCES

- [1] M. Tang, J. Gao, G. Dong, C. Yang, B. Campbell, B. Bowman, J. M. Zoellner, E. Abdel-Rahman, and M. Boukhechba, "Srda: Mobile sensing based fluid overload detection for end stage kidney disease patients using sensor relation dual autoencoder," in *Conference on Health, Inference, and Learning*. PMLR, 2023, pp. 133–146.
- [2] J. Gao, W. Wang, F. Nikseresht, V. Govinda Rajan, and B. Campbell, "Pfdrl: Personalized federated deep reinforcement learning for residential energy management," in *Proceedings of the 52nd International Conference on Parallel Processing*, 2023, pp. 402–411.
- [3] Q. Yang, Y. Liu, T. Chen, and Y. Tong, "Federated machine learning: Concept and applications," *ACM Transactions on Intelligent Systems and Technology (TIST)*, vol. 10, no. 2, pp. 1–19, 2019.
- [4] B. McMahan, E. Moore, D. Ramage, S. Hampson, and B. A. y Arcas, "Communication-efficient learning of deep networks from decentralized data," in *Artificial intelligence and statistics*. PMLR, 2017, pp. 1273–1282.
- [5] T. Li, A. K. Sahu, M. Zaheer, M. Sanjabi, A. Talwalkar, and V. Smith, "Federated optimization in heterogeneous networks," *Proceedings of Machine learning and systems*, vol. 2, pp. 429–450, 2020.
- [6] S. P. Karimireddy, S. Kale, M. Mohri, S. Reddi, S. Stich, and A. T. Suresh, "Scaffold: Stochastic controlled averaging for federated learning," in *International conference on machine learning*. PMLR, 2020, pp. 5132–5143.
- [7] L. G. Anthopoulos, "Understanding the smart city domain: A literature review," *Transforming city governments for successful smart cities*, pp. 9–21, 2015.
- [8] A. L. Virk, M. A. Noor, S. Fiaz, S. Hussain, H. Hussain, M. Rehman, M. Ahsan, and W. Ma, "Smart farming: An overview," *Smart Village Technology*, 2020.
- [9] L. Liu, J. Zhang, S. Song, and K. B. Letaief, "Client-edge-cloud hierarchical federated learning," in *ICC 2020-2020 IEEE international conference on communications (ICC)*. IEEE, 2020, pp. 1–6.
- [10] S. A. Tijani, X. Ma, R. Zhang, F. Jiang, and R. Doss, "Federated learning with extreme label skew: A data extension approach," in *2021 International Joint Conference on Neural Networks (IJCNN)*, 2021, pp. 1–8.
- [11] J. Sheng, J. Xiong, and B. Liu, "Federated learning technology in serial topology for iot networks," *2023 IEEE International Symposium on Broadband Multimedia Systems and Broadcasting (BMSB)*, pp. 1–5, 2023.
- [12] J. Liu, F. Shang, Y. Liu, H. Liu, Y. Li, and Y. Gong, "FedBCGD: Communication-efficient accelerated block coordinate gradient descent for federated learning," in *ACM Multimedia 2024*, 2024. [Online]. Available: <https://openreview.net/forum?id=IAFO0SUjXD>
- [13] Y. Sun, X. Gao, Y. Shen, J. Xie, J. Yang, and N. Si, "A model parameter update strategy for enhanced asynchronous federated learning algorithm," in *2023 IEEE 3rd International Conference on Computer Systems (ICCS)*, 2023, pp. 9–15.
- [14] A. Fallah, A. Mokhtari, and A. Ozdaglar, "Personalized federated learning: A meta-learning approach," *arXiv preprint arXiv:2002.07948*, 2020.
- [15] J. Xu, W. Du, Y. Jin, W. He, and R. Cheng, "Ternary compression for communication-efficient federated learning," *IEEE Transactions on Neural Networks and Learning Systems*, vol. 33, no. 3, pp. 1162–1176, 2022.
- [16] Y. Wang, L. Lin, and J. Chen, "Communication-efficient adaptive federated learning," *ArXiv*, vol. abs/2205.02719, 2022.
- [17] X.-C. Li and D.-C. Zhan, "Fedrs: Federated learning with restricted softmax for label distribution non-iid data," in *Proceedings of the 27th ACM SIGKDD Conference on Knowledge Discovery & Data Mining*, ser. KDD '21. New York, NY, USA: Association for Computing Machinery, 2021, p. 995–1005. [Online]. Available: <https://doi.org/10.1145/3447548.3467254>
- [18] M. G. Arivazhagan, V. Aggarwal, A. K. Singh, and S. Choudhary, "Federated learning with personalization layers," *arXiv preprint arXiv:1912.00818*, 2019.
- [19] G. M. Weiss, K. Yoneda, and T. Hayajneh, "Smartphone and smartwatch-based biometrics using activities of daily living," *Ieee Access*, vol. 7, pp. 133 190–133 202, 2019.
- [20] Z. Yang, Y. Zhang, G. Zhang, Y. Zheng, and G. Chi, "Widar 3.0: Wifi-based activity recognition dataset," 2020. [Online]. Available: <https://dx.doi.org/10.21227/7znf-qp86>
- [21] Y. Zheng, Y. Zhang, K. Qian, G. Zhang, Y. Liu, C. Wu, and Z. Yang, "Zero-effort cross-domain gesture recognition with wi-fi," in *Proceedings of the 17th annual international conference on mobile systems, applications, and services*, 2019, pp. 313–325.
- [22] J. W. Lockhart, G. M. Weiss, J. C. Xue, S. T. Gallagher, A. B. Grosner, and T. T. Pulickal, "Design considerations for the wisdm smart phone-based sensor mining architecture," in *Proceedings of the Fifth International Workshop on Knowledge Discovery from Sensor Data*, 2011, pp. 25–33.
- [23] Y. LeCun, L. Bottou, Y. Bengio, and P. Haffner, "Gradient-based learning applied to document recognition," *Proceedings of the IEEE*, vol. 86, no. 11, pp. 2278–2324, 1998.
- [24] Q. Li, Y. Diao, Q. Chen, and B. He, "Federated learning on non-iid data silos: An experimental study," in *2022 IEEE 38th international conference on data engineering (ICDE)*. IEEE, 2022, pp. 965–978.
- [25] A. F. Aji and K. Heafield, "Sparse communication for distributed gradient descent," *arXiv preprint arXiv:1704.05021*, 2017.
- [26] R. A. Sekar, T. Prabakaran, A. Sudhakar, and R. S. Kumar, "Industrial automation using iot," in *AIP Conference Proceedings*, vol. 2393, no. 1. AIP Publishing, 2022.
- [27] H. H. Nguyen, F. Mirza, M. A. Naeem, and M. Nguyen, "A review on iot healthcare monitoring applications and a vision for transforming sensor data into real-time clinical feedback," in *2017 IEEE 21st International Conference on Computer Supported Cooperative Work in Design (CSCWD)*, 2017, pp. 257–262.
- [28] A. Imteaj, U. Thakker, S. Wang, J. Li, and M. Amini, "A survey on federated learning for resource-constrained iot devices," *IEEE Internet of Things Journal*, vol. 9, pp. 1–24, 2021.
- [29] X. Wu, X. Yao, and C.-L. Wang, "Fedscr: Structure-based communication reduction for federated learning," *IEEE Transactions on Parallel and Distributed Systems*, vol. 32, no. 7, pp. 1565–1577, 2021.
- [30] M. Nori, S. Yun, and I. Kim, "Fast federated learning by balancing communication trade-offs," *IEEE Transactions on Communications*, vol. 69, pp. 5168–5182, 2021.
- [31] J. ji Ren, W. Ni, and H. Tian, "Toward communication-learning trade-off for federated learning at the network edge," *IEEE Communications Letters*, vol. 26, pp. 1858–1862, 2022.
- [32] Y. Cui, K. Cao, G. Cao, M. Qiu, and T. Wei, "Client scheduling and resource management for efficient training in heterogeneous iot-edge federated learning," *IEEE Transactions on Computer-Aided Design of Integrated Circuits and Systems*, vol. 41, no. 8, pp. 2407–2420, 2022.
- [33] C. Briggs, Z. Fan, and P. Andras, "Federated learning with hierarchical clustering of local updates to improve training on non-iid data," in *2020 International Joint Conference on Neural Networks (IJCNN)*, 2020, pp. 1–9.
- [34] T. Liu, J. Ding, T. Wang, M. Pan, and M. Chen, "Towards fast and accurate federated learning with non-iid data for cloud-based iot applications," *Journal of Circuits, Systems and Computers*, vol. 31, no. 13, p. 2250235, 2022. [Online]. Available: <https://doi.org/10.1142/S0218126622502358>
- [35] H. Zhou, J. Lan, R. Liu, and J. Yosinski, "Deconstructing lottery tickets: Zeros, signs, and the supermask," *Advances in neural information processing systems*, vol. 32, 2019.
- [36] Y. Bengio, N. Léonard, and A. Courville, "Estimating or propagating gradients through stochastic neurons for conditional computation," *arXiv preprint arXiv:1308.3432*, 2013.
- [37] P. A. Ferreira, P. N. da Silva, V. Gottin, R. Stelling, and T. Calmon, "Bayesian signsgd optimizer for federated learning," *Advances in Neural Information Processing Systems*, vol. 34, 2021.
- [38] N. Ravi, N. Dandekar, P. Mysore, and M. L. Littman, "Activity recognition from accelerometer data," in *Aaai*, vol. 5, no. 2005. Pittsburgh, PA, 2005, pp. 1541–1546.
- [39] J.-L. Reyes-Ortiz, L. Oneto, A. Samà, X. Parra, and D. Anguita, "Transition-aware human activity recognition using smartphones," *Neurocomputing*, vol. 171, pp. 754–767, 2016.
- [40] C. A. Ronao and S.-B. Cho, "Human activity recognition with smartphone sensors using deep learning neural networks," *Expert systems with applications*, vol. 59, pp. 235–244, 2016.
- [41] S. Purohit *et al.*, "Evaluation of the efficacy of iot deployment on petro-retail operations," *Turkish Journal of Computer and Mathematics Education (TURCOMAT)*, vol. 12, no. 4, pp. 356–363, 2021.